

# Clustered star formation

Jonathan P. Williams

Institute for Astronomy, University of Hawaii, Honolulu, HI 96822 USA  
email: jpw@ifh.hawaii.edu

**Abstract.** Most stars, including all massive stars, form in clusters. Here, I present (sub-)millimeter observations of young stellar clusters in two well known massive star forming regions. First, I discuss relatively low mass cluster formation across the Rosette molecular cloud and the influence of the OB association, NGC 2244 (the Rosette nebula) on their properties. Second, I present SMA observations of the Trapezium cluster in Orion and the detection of emission from protoplanetary disks (proplyds) around 4 low mass stars. The implications for Solar System scale planet formation around low mass stars in high mass star forming environments are discussed.

**Keywords.** stars: formation, ISM: clouds, ISM: kinematics and dynamics, ISM: molecules, submillimeter

---

## 1. Introduction

Massive stars form in large groups in Giant Molecular Clouds (GMCs). Understanding their formation, therefore, requires extending our knowledge of isolated star formation to the more common mode of cluster formation, and learning about the structure and dynamics of turbulent clouds relative to thermal cores. Most low mass stars are also born in OB associations and a related issue of great significance is understanding disk evolution and the possibilities for planet formation in such conditions. In this talk, I present early results from work in these two broad areas.

## 2. Cluster formation across the Rosette molecular cloud

I began studying the Rosette molecular cloud for my thesis and, like a bad dose of the flu, have not been able to shake it. As with almost all areas of science, technology keys progress and the 32-element, broadband SEQUOIA receiver on the FCRAO 14 m telescope was able to map out the entire cloud ( $\sim 4$  square degrees) simultaneously in the 1–0 transition of CO and  $^{13}\text{CO}$  in less than two weeks of telescope time. The resolution, coverage, and sensitivity are all substantially greater in these maps than those shown in Figure 1 from Williams, Blitz, & Stark (1995).

Cloud structure analysis has also become more sophisticated than clump-finding algorithms (Williams, de Geus, & Blitz 1994). Using Principal Component Analysis (Heyer & Schloerb 1997), it is possible to compare the turbulent conditions of the cloud from near the HII region, NGC 2244, to that far away. The new FCRAO maps and analysis will be presented in Heyer, Williams, & Brunt (2005).

A comparison of the optically thick CO and optically thinner  $^{13}\text{CO}$  maps show that there is substantial warm molecular gas in the region, that the temperature drops off toward the far end of the cloud away from the nebula, but that most of the column density (and therefore mass) lies near the midplane of the cloud.

The decrease in temperature across the cloud is similar to that expected for a blackbody illuminated by a point source,  $T^4 \propto 1/d^2$  (Figure 2). This suggests that the gas is well coupled to the dust and that the bulk of the cloud is heated by the radiation from the 17

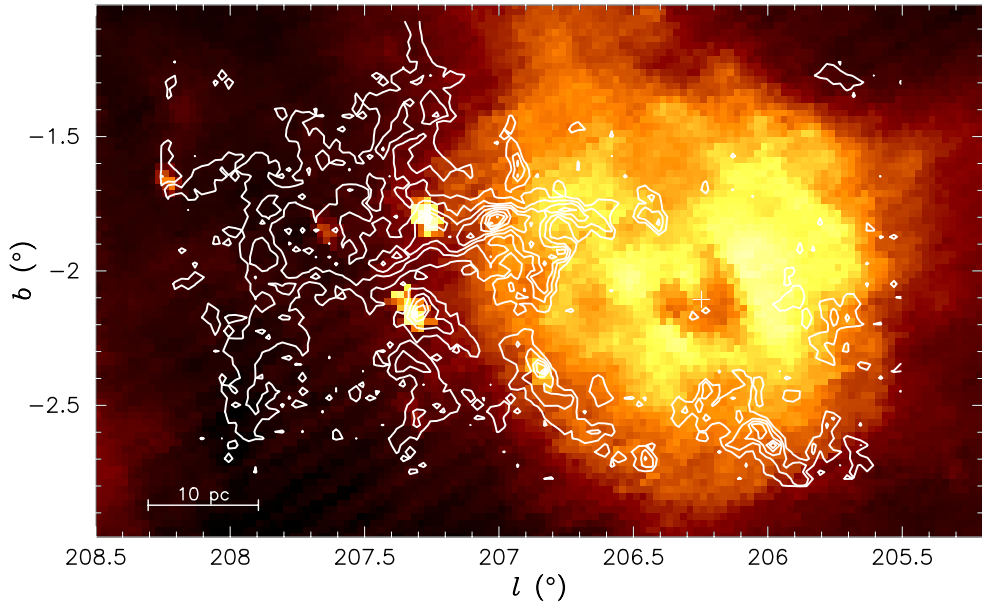


**Figure 1.** Contours of integrated CO(1–0) emission in the Rosette molecular cloud, shown overlaid on a ratio map of IRAS 60 to 100 microns. The former shows the location of the molecular gas, the latter the location of warm dust both from the Rosette nebula (centered at the cross near  $l = 206.4$ ,  $b = -2.1$ ) and new regions of star formation embedded within the cloud (e.g.  $l = 207.3$ ,  $b = -1.7$ ,  $-2.1$ ).

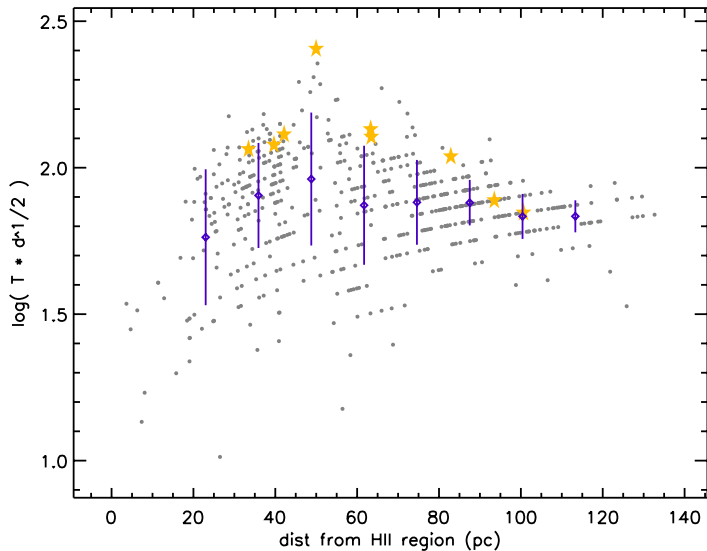


**Figure 2.** Temperature variation across the Rosette molecular cloud. The dots show a combination of the CO peak temperature and distance from the HII region for clumps in the cloud. The vertical bars show averages and dispersions in distance bins and the stars show those clumps with IRAS sources indicative of embedded star formation.

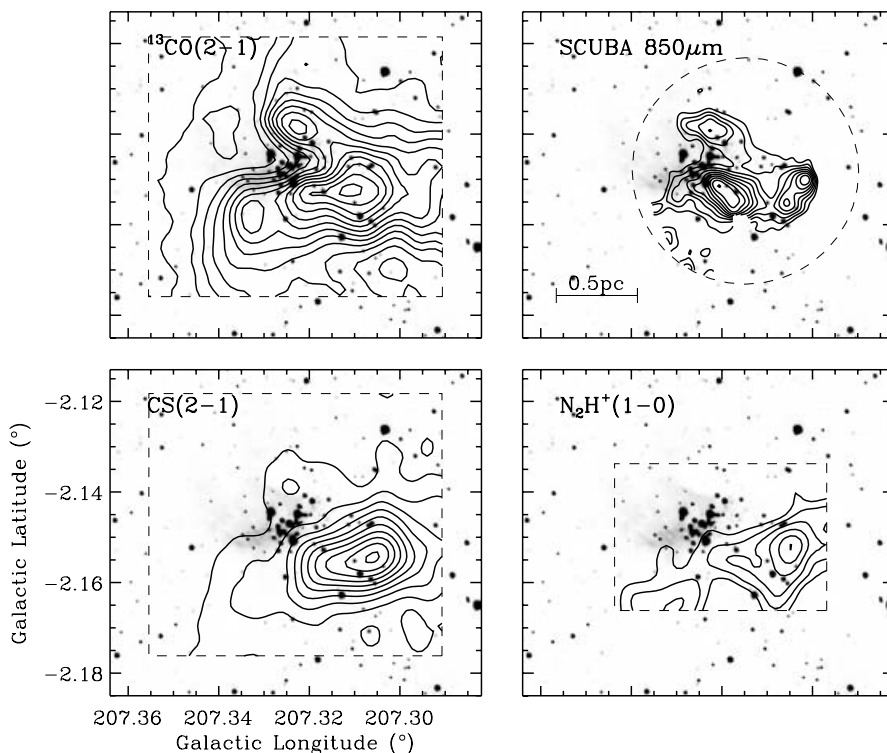


**Figure 3.** Gas and dust toward a cluster in the Rosette molecular cloud. The upper left panel shows  $^{13}\text{CO}$  emission outlining the relatively low density gas, the upper right panel shows the total dust column density, and the bottom panels show CS and  $\text{N}_2\text{H}^+$  emission from dense gas. The cluster is breaking out of its molecular envelope which breaks up into three main clumps each with a distinct chemistry. Faint red sources, perhaps newly formed stars, are found in the west most cluster where there is strong dense gas emission.

O and B stars in the Rosette nebula. The IRAS Point Source Catalog reveals embedded sites of star formation across the cloud (Cox *et al.* 1990) and these provide some localized heating in addition to the general trend in Figure 2. Given that the stars in the nebula dominate the heating of the cloud, however, the question naturally arises as to whether they also influence the star formation within it.

There is substantial mass in relatively cold material away from the HII region. There is also some star formation there but the luminosity of the IRAS sources is  $\sim 50$  times lower than the bright central sources in the cloud. Near-infrared imaging shows that each IRAS source is a small cluster of young stars (Phelps & Lada 1997). More recent, deeper, wide field imaging with the new FLAMINGOS camera reveals the stellar population of these clusters down to the brown dwarf limit. The analysis of these data is the subject of Carlos Roman's PhD thesis (Univ. Florida). From the colors, K-band luminosity, and spectroscopy, it is hoped that cluster masses and ages will be measured across the cloud.

We have mapped the dust and gas in the clumps forming the clusters using SCUBA on the JCMT and the heterodyne receivers on the IRAM 30 m. The dust images are the most unbiased measures of the mass and its distribution. This is generally well correlated with the central peak of the near-infrared clusters. In some cases, however, there are secondary

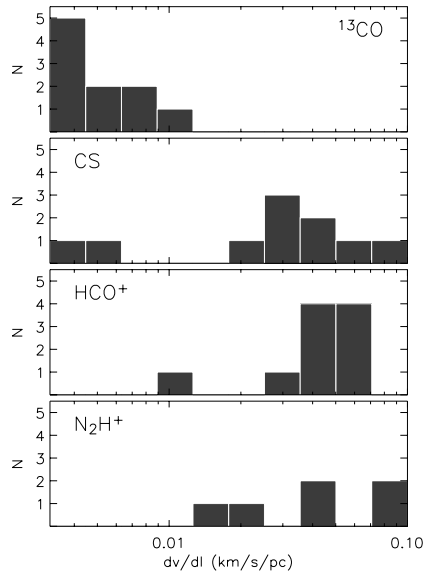


**Figure 4.** Velocity gradients for 10 cluster forming clumps in the Rosette cloud. There is little or no velocity pattern in  $^{13}\text{CO}$  which traces the low density outer envelopes of the clumps. The motions become more ordered in the inner regions at higher densities, traced by CS,  $\text{HCO}^+$ , and  $\text{N}_2\text{H}^+$  (for which only 6 clumps were mapped).

peaks offset from the center where faint K-band sources are found. These red sources may be highly reddened, deeply embedded and potentially very young objects (Figure 3).

The IRAM line data shows the chemistry and dynamics of the cluster forming clumps. We find that line wing emission in CO from poorly collimated outflows in a few cases.  $^{13}\text{CO}$  and  $\text{C}^{18}\text{O}$  maps are similar to the SCUBA maps and therefore likely to be fairly reliable mass tracers. CS and  $\text{N}_2\text{H}^+$  are good tracers of the denser gas that is more closely associated with star formation. These two tracers also correlate quite closely. The situation is somewhat different than in low mass isolated star forming cores where the CS depletes toward the center, perhaps because of the higher temperatures in these cluster forming regions.

We searched for signs of inward motions due to red-shifted self-absorption in each core but found none. Again, this is different from low mass cores where self-absorbed line profiles in dense gas tracers are quite common (e.g. Lee, Myers, & Tafalla 1999). This may be due to the more turbulent nature of the cluster forming cores, a shallower excitation gradient, a shallower abundance gradient, or some combination thereof. It is probably not due to resolution as self-absorbed profiles can extend over  $\sim 0.1$  pc, greater than the IRAM beamsize in the Rosette. The lack of self-absorbed profiles is not restricted to the Rosette as a survey of other cluster forming regions also showed a small percentage of infall candidates (Williams & Myers 1999).

As the line profiles were nearly gaussian in most cases, there was not ambiguity about measuring the systemic motions in the clumps. We found that the CO lines which trace relatively low density gas, showed little or no clear velocity patterns but that CS,  $\text{HCO}^+$ , and  $\text{N}_2\text{H}^+$  which are excited by the higher density inner regions of the clumps, show much more organized motions with clear velocity gradients ranging from  $\sim 0.03$  to  $\sim 0.1 \text{ km s}^{-1} \text{ pc}^{-1}$ . This is shown graphically in Figure 4 and suggests a turbulent outer

envelope with a denser center where the (still supersonic) motions are more organized. This is somewhat reminiscent of a “transition to coherence” seen in low mass cores by Goodman *et al.* (1998) but at larger spatial and velocity scales.

A thorough analysis and writeup of the FLAMINGOS near-infrared cluster mapping and the IRAM observations of their envelopes is well underway and will be published by Carlos Roman shortly.

### 3. Can planetary systems form in the Trapezium cluster?

Given that most low mass stars are born in OB associations (McKee & Williams 1997), it is essential to understand their formation in such an environment. As the statistics of extrasolar planetary systems become better understood (e.g. Marcy, Cochran, & Mayor 2000), it is also natural to extend this question to the formation of planets around low mass stars in massive star forming regions.

The Trapezium cluster in Orion is the nearest young, massive star forming region and it is consequently the most intensively studied (e.g. O’Dell 2001). There are approximately  $10^3 \sim 1$  Myr old stars in the central 1 pc of the cluster core (Hillenbrand 1997) but the radiation field is dominated by one O6 star,  $\theta^1$  Ori C. Ionized gas from the evaporating envelopes and disks around nearby low mass stars can be observed at centimeter wavelengths with the VLA (Churchwell *et al.* 1987) through the optical, most spectacularly with HST (beginning with O’Dell, Wen & Hu 1993).

The HST images provide some of the most dramatic images of protostellar disks that exist (see in particular Bally *et al.* 1998a). They were dubbed “proplyds” by O’Dell as they were presumed to be protoplanetary on account of their solar system scale sizes. However their masses – and potential for forming planets – were unknown. Only a lower limit less than a Jupiter mass could be obtained by integrating a minimal extinction over their area (McCaughrean *et al.* 1998) and it was not clear, therefore, that the proplyds had enough mass to form (giant) planets.

Disk masses are best measured at longer wavelengths where the dust emission becomes optically thin. Interferometry is essential to resolve the tightly clustered proplyds from each other and also to filter out the strong emission from the background molecular cloud. Mundy, Looney, & Lada (1995) used the BIMA interferometer at  $\lambda 3.5$  mm to image a field around  $\theta^1$  Ori C containing 33 proplyds. Several significant peaks were found, four coincident with proplyds, but the intensity was consistent with free-free emission from ionized gas and they were unable to measure masses. By analyzing the non-detections, however, they were able to place a statistical upper limit of  $0.03 M_{\odot}$  on the average disk mass. The dust emission increases at shorter wavelengths and the free-free emission decreases. Using the OVRO array, Bally *et al.* (1998b) imaged two fields containing a total of six proplyds at  $\lambda 1.3$  mm, made a tentative detection of one object with a mass equal to  $0.02 M_{\odot}$ , and placed upper limits of  $0.015 M_{\odot}$  on the other objects. Lada (1999) presented a mosaic of two fields at  $\lambda 1.3$  mm with the Plateau de Bure interferometer that claimed three detections. The implied masses were  $\sim 0.01 M_{\odot}$  but these have not been analyzed in detail.

By operating at shorter wavelengths than the other interferometers, the Submillimeter Array (SMA; Ho *et al.* 2004) is better suited to measuring the dust emission above the strong bremsstrahlung emission from the ionized gas. Furthermore, it has a relatively large field of view which allows many proplyds to be imaged simultaneously.

Details of the observations and their analysis are in Williams, Andrews, & Wilner (2005). We observed a single field toward the center of the Trapezium cluster at 340 GHz ( $880 \mu\text{m}$ ). 23 proplyds were contained within the  $32''$  full width half maximum primary

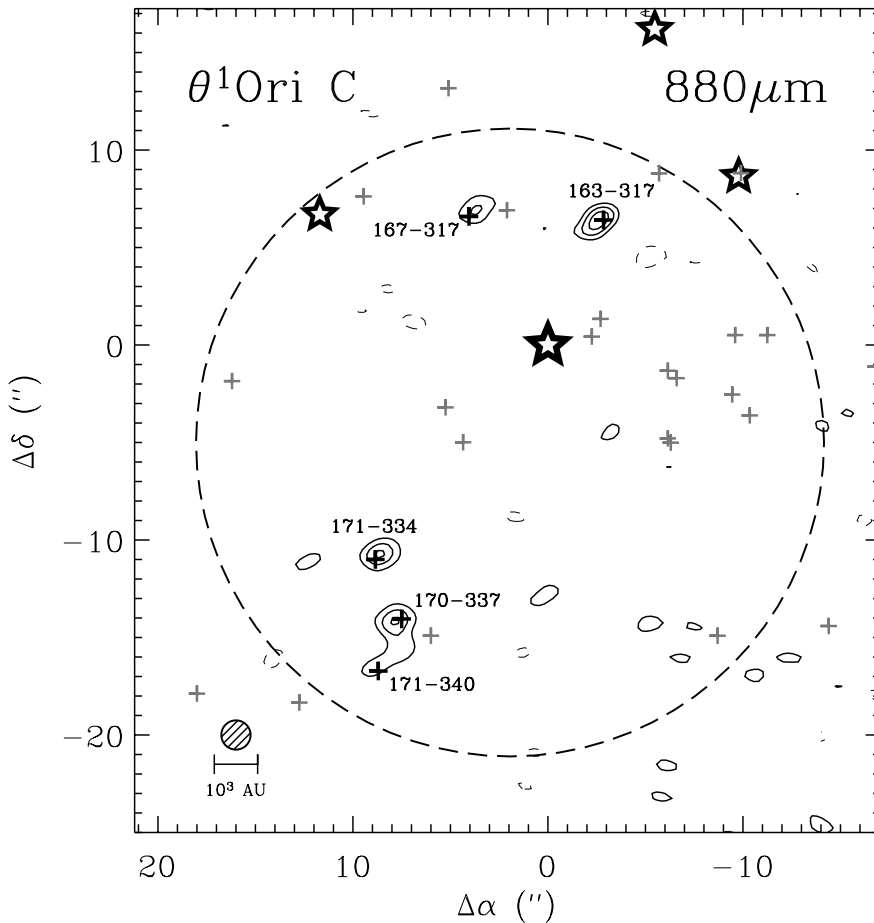


**Figure 5.** Contours of  $880\ \mu\text{m}$  continuum emission toward the proplyds in the Trapezium cluster. The locations of the proplyds from O'Dell & Wen (1994) are shown by crosses and the five detections are labeled following their nomenclature. The position of the four Trapezium O stars are shown by the large star symbols and the center of the coordinate grid has been set to  $\theta^1$  Ori C. The  $1.5''$  synthesized beam and scale bar are shown in the lower left corner, the large dashed circle is the FWHM of the primary beam. Contour levels are at  $3, 5, 7 \times \sigma$  where  $\sigma = 2.7\ \text{mJy beam}^{-1}$  is the rms noise level in the map.

beam. The resolution of these compact configuration data was  $1.5''$  and the rms noise level was  $\sigma = 2.7\ \text{mJy beam}^{-1}$ .

Contours of the continuum emission are shown in Figure 5. Five proplyds were detected within the  $32''$  FWHM of the primary beam with a peak flux greater than  $3\sigma = 8.1\ \text{mJy beam}^{-1}$  and are labeled in the Figure. 167-317 ( $\theta^1$  Ori G) is a very bright source in the optical and radio. Based on an extrapolation of its SED at centimeter wavelengths (Garay, Moran, & Reid 1987), we appear to be detecting the bremsstrahlung emission from its ionized cocoon even at these short wavelengths. The four other proplyds have fluxes that are significantly above the bremsstrahlung extrapolation and we attribute the bulk of the SMA flux to thermal dust emission.

The corresponding disk masses for these four proplyds, after correcting for a contribution from ionized gas, range from  $1.3$  to  $2.4 \times 10^{-2}\ M_{\odot}$ . These are similar to the

minimum mass solar nebula (Weidenschilling 1977). Photo-evaporative mass loss rates are high,  $\sim 10^{-7} M_{\odot} \text{ yr}^{-1}$  (Churchwell *et al.* 1987), but concentrated in the outer parts of the disks where the gravitational potential of the central star is weakest and photo-evaporation is most effective (Hollenbach, Yorke, & Johnstone 2000). The radius of the bound inner region depends on the stellar mass and whether the gas is ionized by EUV photons or remains neutral and only heated by the FUV radiation field. The detected proplyds lie far enough away from  $\theta^1$  Ori C for the second condition to apply and the central  $\sim 20$ – $50$  AU radius of the disks survive (Johnstone *et al.* 1998). Disk radii, measured from the HST observations, are  $\sim 40$  AU for the detections so, at most, only the outer 50% of the disk will be lost. For a surface density  $\Sigma \sim r^{-3/2}$ , the surviving mass fraction is at least 60%. In these systems at least, the submillimeter emission indicates there is sufficient material bound to the star to form Solar System scale planetary systems.

### Acknowledgements

I thank the organizers of this meeting for inviting me. Several students, Meredith Hughes, Sandrine Bottinelli, Carlos Roman, and Sean Andrews have been involved in this work which is supported by the NSF under grant AST-0324328. Big props also to my more senior collaborators, Mark Heyer, Chris Brunt, and David Wilner.

### References

- Bally, J., Sutherland, R. S., Devine, D., & Johnstone, D. 1998a, *AJ*, 116, 293  
 Bally, J., Testi, L., Sargent, A., & Carlstrom, J. 1998b, *AJ*, 116, 854  
 Churchwell, E., Felli, M., Wood, D. O. S., & Massi, M. 1987, *ApJ*, 321, 516  
 Cox, P., Deharveng, & Leene 1990, *A&A*, 230, 181  
 Garay, G., Moran, J. M., & Reid, M. J. 1987, *ApJ*, 314, 535  
 Goodman, A. A., Barranco, J. A., Wilner, D. J., & Heyer, M. H. 1998, *ApJ*, 504, 223  
 Hillenbrand, L. A. 1997, *AJ*, 113, 1733  
 Ho, P. T. P., Moran, J. M., & Lo, K. Y. 2004, *ApJ*, 616, L1  
 Hollenbach, D. J., Yorke, H. W., & Johnstone, D. 2000, *Protostars and Planets IV*, 401  
 Johnstone, D., Hollenbach, D., & Bally, J. 1998, *ApJ*, 499, 758  
 Lada, E. A. 1999, *NATO ASIC Proc. 540: The Origin of Stars and Planetary Systems*, 441  
 Lee, C. W., Myers, P. C., & Tafalla, M. 1999, *ApJ*, 526, 788  
 Marcy, G. W., Cochran, W. D., & Mayor M. 2000, *Protostars and Planets IV*, 1285  
 McCaughrean, M. J., *et al.* 1998, *ApJ*, 492, 157  
 McKee, C. F., & Williams, J. P. 1997, *ApJ*, 476, 144  
 Mundy, L. G., Looney, L. W., & Lada, E. A. 1995, *ApJ*, 452, L137  
 O'Dell, C. R. 2001, *ARAA*, 39, 99  
 O'Dell, C. R., Wen, Z., & Hu, X. 1993, *ApJ*, 410, 696  
 Phelps, R. L., & Lada, E. A. 1997, *ApJ*, 477, 176  
 Weidenschilling, S. J. 1977, *ApJS*, 51, 153  
 Williams, J. P., & Myers, P. C. 1999, *ApJ*, 511, 208  
 Williams, J. P., Andrews, S. M., & Wilner, D. J. 2005, *ApJ*, in press